



# SH21D-2557: CONSTRAINING KAPPA DISTRIBUTION IN ACTIVE REGIONS AT THE SUN USING MICROWAVE GYRORESONANT RADIATION

Gregory Fleishman<sup>1</sup>, Skanda Rao<sup>2</sup>, Ethan Cheung<sup>2</sup>,  
Gelu Nita<sup>1</sup>, Alexey Kuznetsov<sup>3</sup>

<sup>1</sup>New Jersey Institute of Technology, Newark, NJ  
<sup>2</sup>Union County Magnet High School, Scotch Plains, NJ  
<sup>3</sup>Institute of Solar-Terrestrial Physics, Irkutsk, Russia

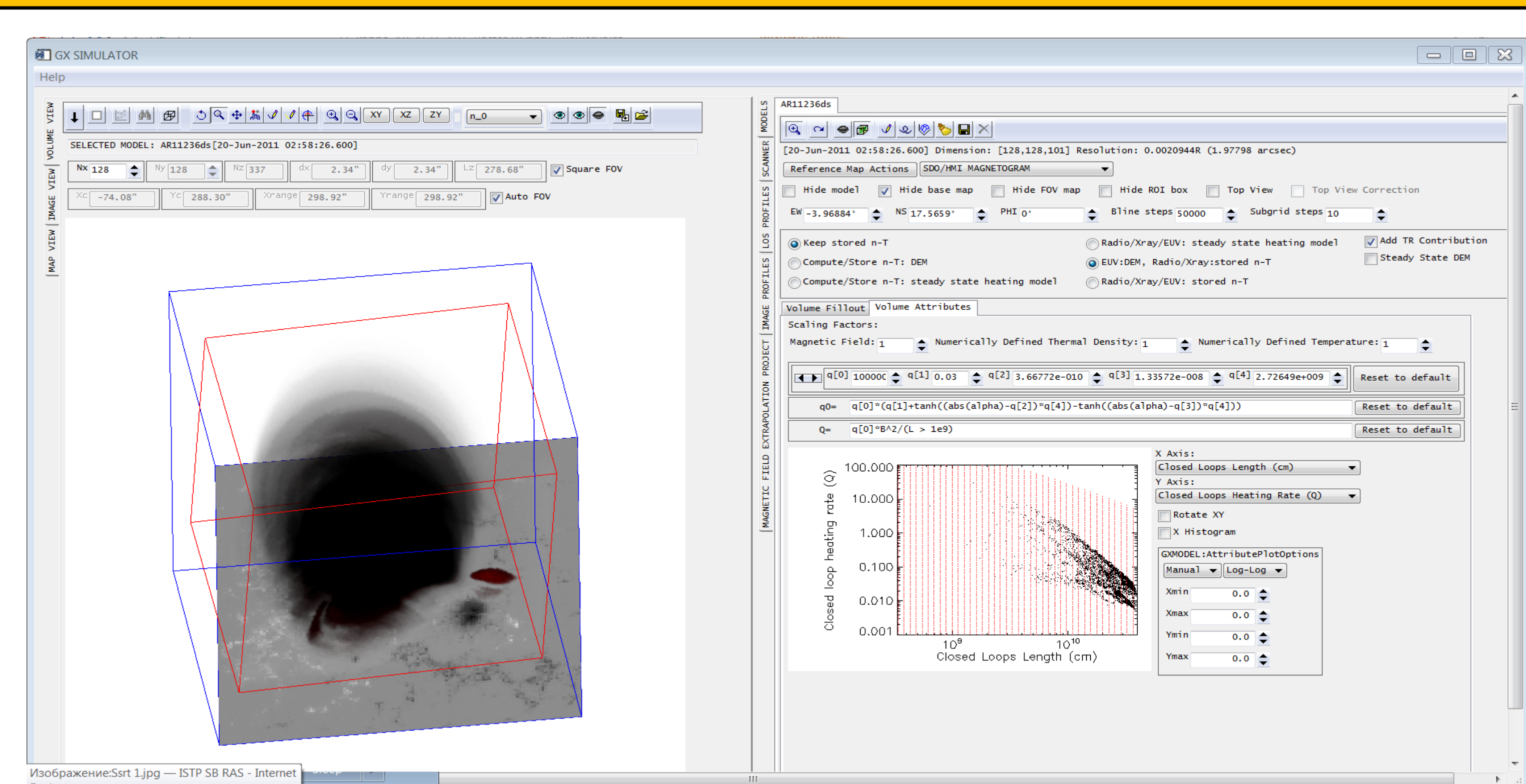
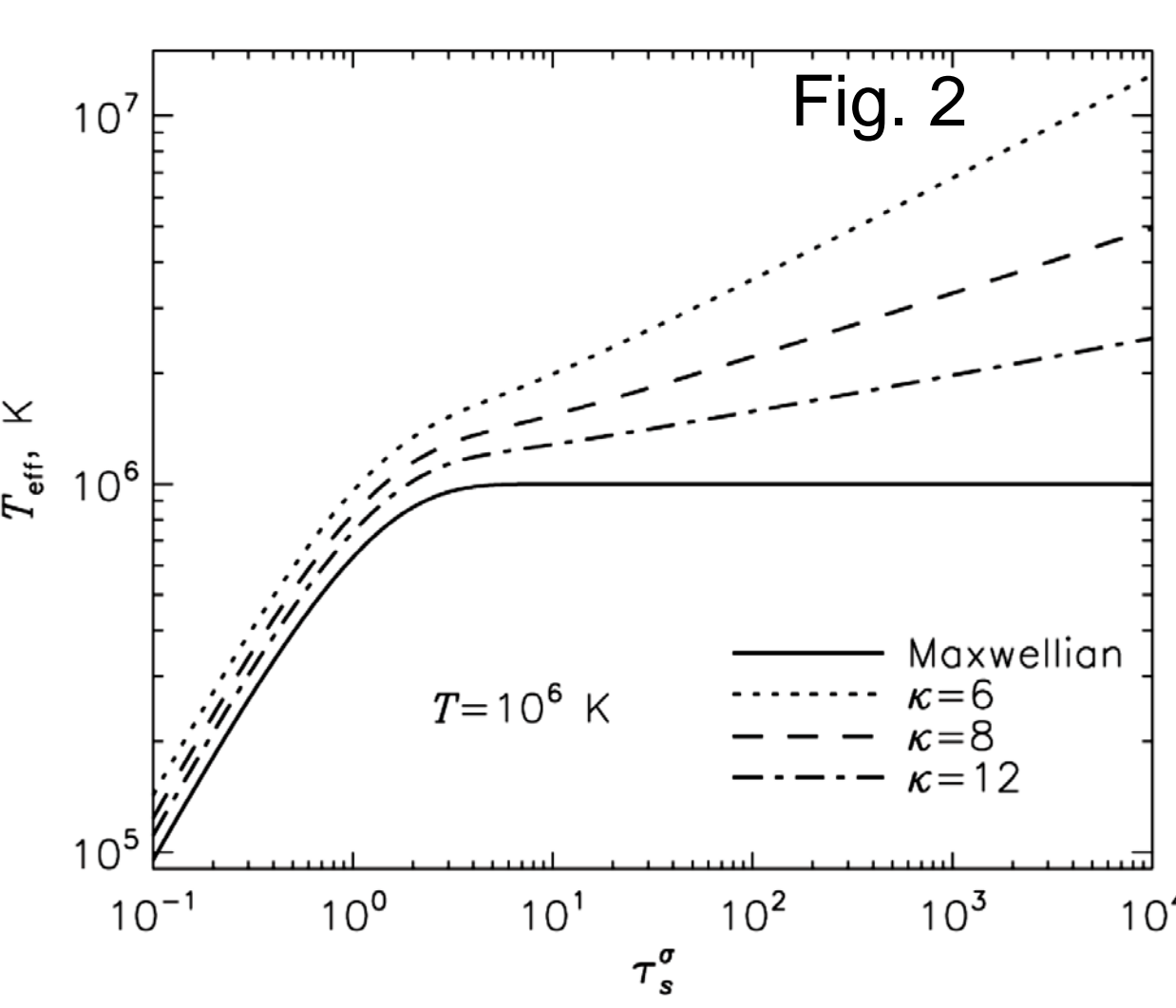
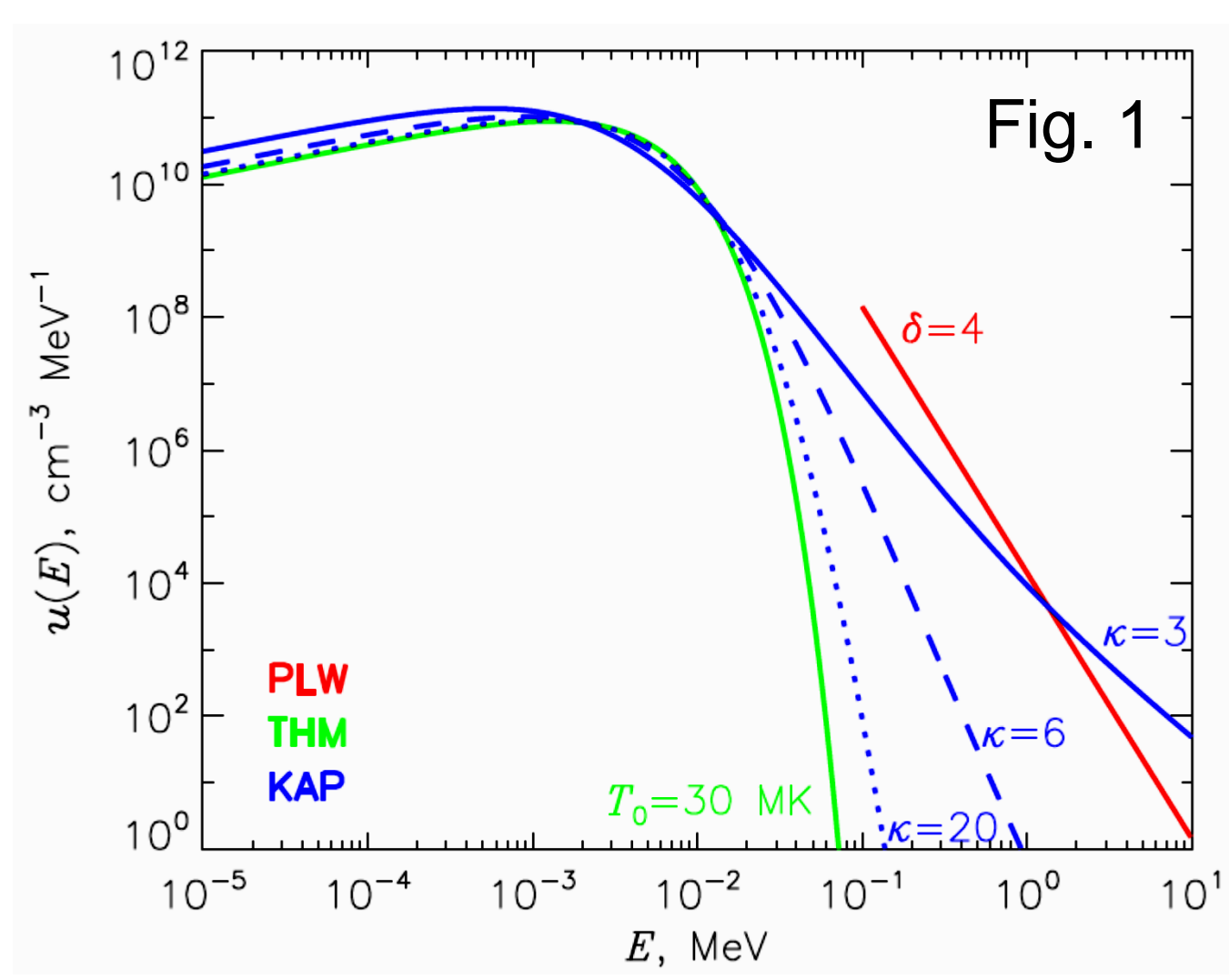


## ABSTRACT

Typically, the distribution function of an astrophysical plasma in a steady state is assumed to be Maxwellian. However, for many observations the Maxwellian distribution is hardly distinguishable from the kappa distribution with a reasonably large index, say kappa=10. Interestingly, in case of plasma with the kappa distribution, the microwave gyroresonance (GR) emission with its large optical depth is extraordinarily sensitive to the kappa index value, because the optically thick emission is highly sensitive to small variations at the tail of the distribution. Here, to constrain possible values of the kappa index in the thermal plasmas of solar corona we consider GR emission from solar active regions using 3D modeling enabled by GX Simulator modeling tool. The 3D magnetic structure is modeled using nonlinear force-free field extrapolation from photospheric vector magnetic field data available from SDO/HMI. Then, this magnetic skeleton is filled with a thermal plasma (n and T values in each voxel of the 3D model) in such a way that the EUV emission computed from the model agrees quantitatively (on average) with the EUV emission observed with SDO/AIA. At the next step we adopt these n and T pair obtained from the comparison with the optically thin EUV data, but allow a kappa distribution with unknown index rather than the Maxwellian distribution. In our study we vary the kappa index and compute the radio brightness and polarization maps from the same 3D model using theory developed by Fleishman & Kuznetsov (2014). These synthetic maps are convolved with the point spread function of a given radio interferometer and compared with the observed radio brightness maps. The synthetic radio brightness and the degree of polarization both increase rapidly as the kappa index decreases, which allows, perhaps, the ever most stringent constraints on the kappa-indices consistent with the data. For this study we selected two solar active regions, one bipolar and one unipolar, and found that the allowable kappa indices are in both cases well above the value around 12. We discuss implications of this finding and potential ways to further constrain the kappa distribution shape in the solar plasma.

**Kappa-Distribution and Gyroresonant Emission.** Kappa-distribution generalizes the Maxwellian one by adding one more parameter, index  $\kappa$ , that provides an extra degree of freedom to describe a power-law-like high-energy tail. The larger the kappa-index the closer the kappa-distribution to the Maxwellian one, Fig. 1.

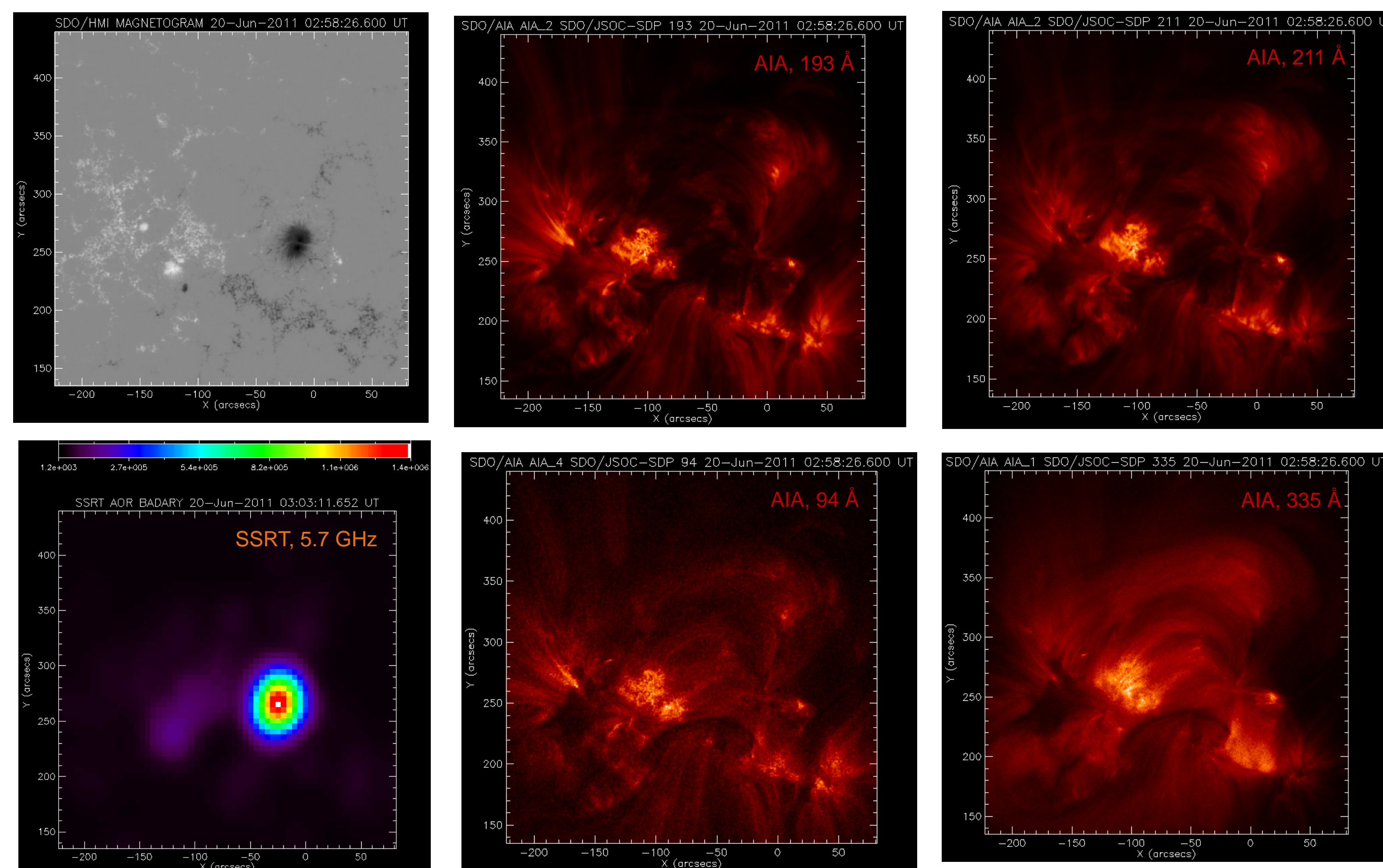
Fleishman & Kuznetsov (2014) demonstrated that the brightness temperature of the GR emission from a gyrolayer will depend now on the total optical depth of the gyrolayer. Figure 2 displays this dependence for the kappa-distribution with different indices. In contrast with the Maxwellian plasma, for which the brightness temperature is just equal to the plasma kinetic temperature for  $\tau > 1$ , the *brightness temperature of the GR emission from a kappa plasma continues to grow with the optical depth  $\tau$* . Not surprisingly, this growth is more pronounced for smaller kappa-indices, i.e., for a stronger departure of the plasma from the Maxwellian distribution. The brightness temperature can exceed the kinetic temperature of the kappa plasma by an order of magnitude or even more for a realistic set of parameters.



IDL-based simulation tool, **GX Simulator** (Nita et al. 2015), is developed for modeling various kinds of emission (Fleishman & Kuznetsov 2010, 2014). The object-based architecture provides an interactive graphical user interface that allows the user (i) to import photospheric magnetic field maps and perform magnetic field extrapolations or import externally generated 3D magnetic field models, (ii) to investigate the magnetic topology of these models by interactively creating magnetic field lines and associated magnetic flux tubes, (iii) to populate the volume and the flux tubes with user-defined nonuniform chromospheric or coronal thermal plasma and anisotropic, nonuniform, nonthermal electron distributions; and (iv) to compute microwave, mm, sub-mm, EUV, and X-ray radiations.

## AR 11236, 20-jun-2011

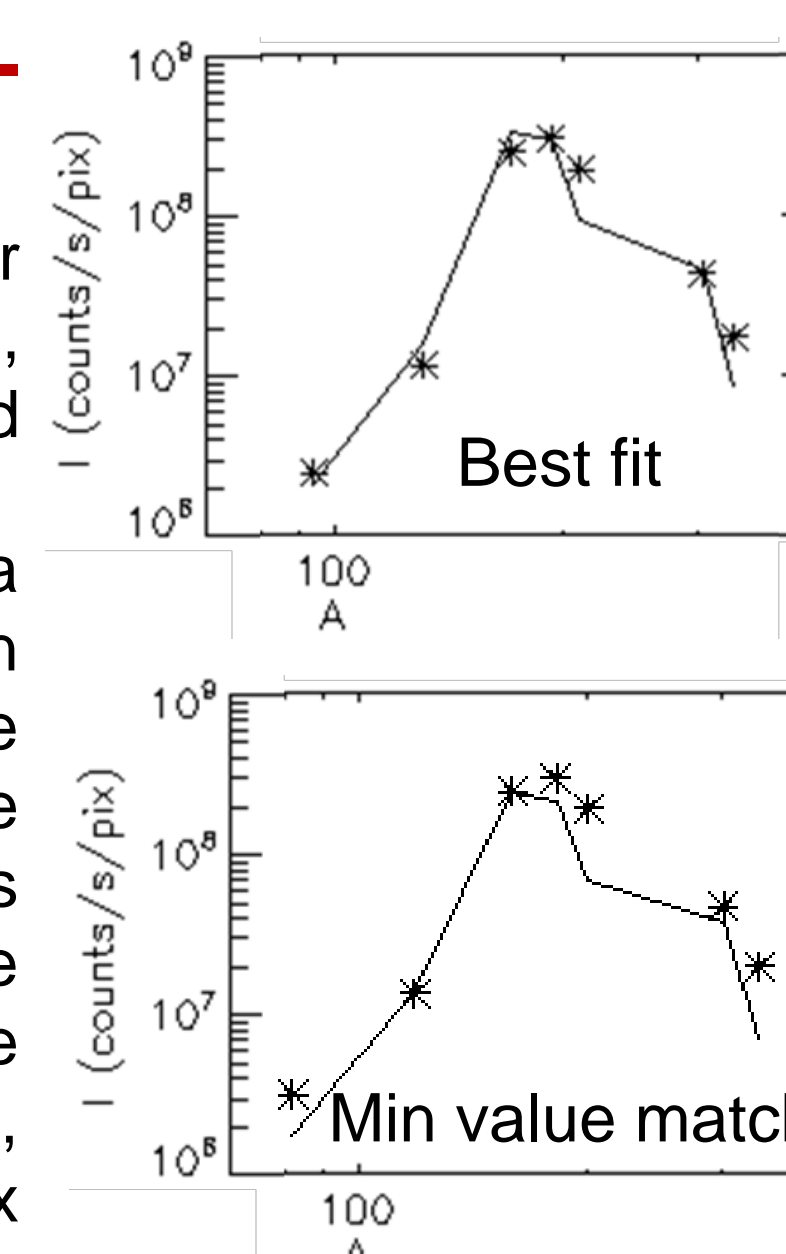
This set of plots represents the photospheric LOS magnetogram from SDO/HMI, four EUV images at 131, 193, 94, 335 Å from SDO/AIA, and microwave image at 5.7 GHz from Siberian Solar Radio Telescope (SSRT).



## How to distinguish between the Maxwellian and kappa-distribution in the coronal plasma?

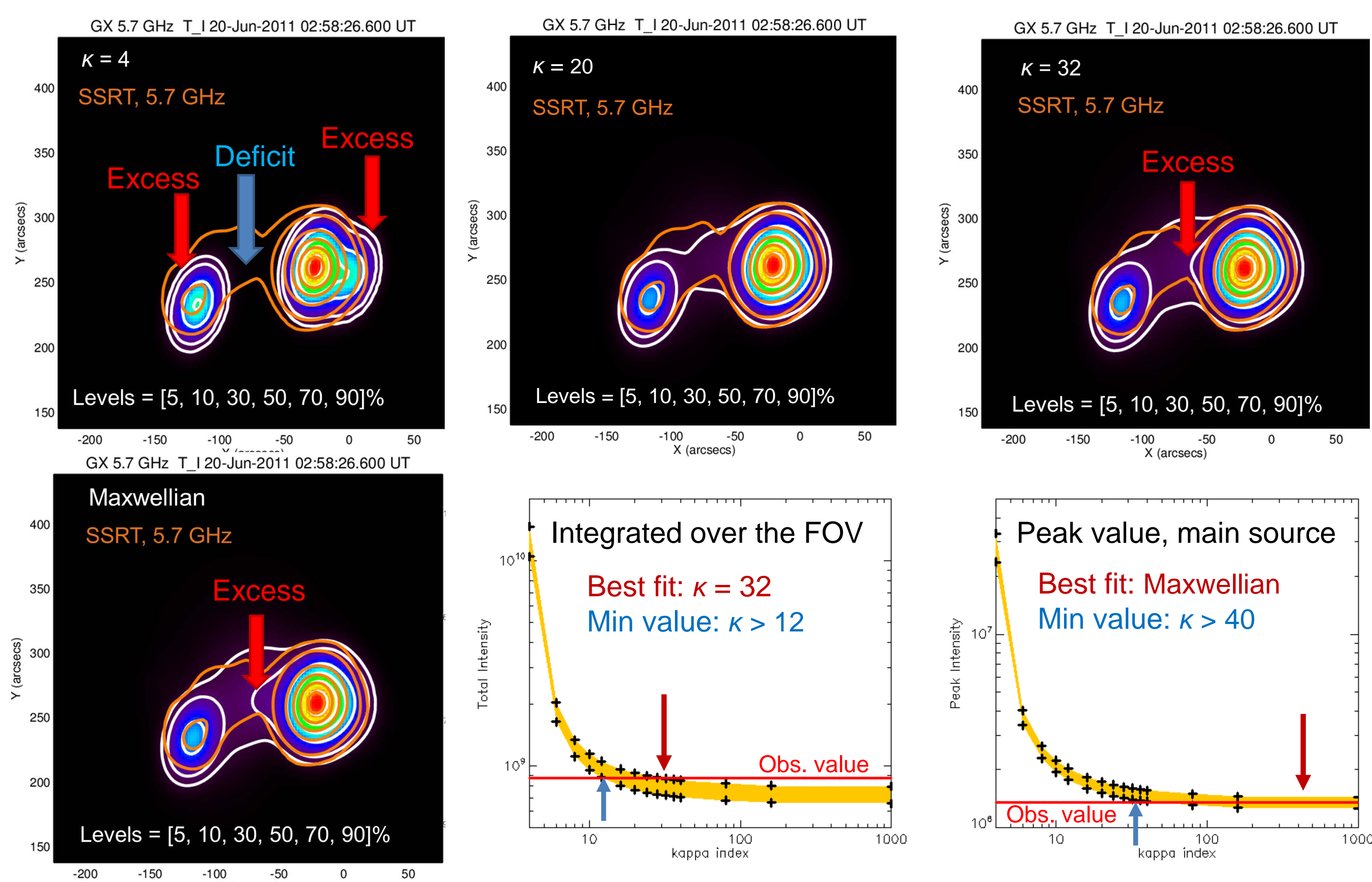
In this study we start from photospheric magnetic vector data and employ a nonlinear force-free field extrapolation using Wiegmann's code (courtesy of Ju Jing). Then, we compute field lines crossing each voxel (3D pixel) in the magnetic data cube and compute length and mean magnetic fields of these field lines.

These quantities are then used to populate each voxel with a thermal plasma described by its own DEM taken from a customized EBTEL runs, which depends on the characteristic heating rate in this active region, which is a free parameter of the model and has to be determined by comparison with observations. To do so we integrate the observed EUV brightness from AIA images and attempt to fit this 'spectrum' (or match the data from below) with the corresponding model outcome such as shown in the top (bottom) Figure (asterisks show the data, line shows the model). As soon as the thermal model is validated via the model-to-data comparison, we compute microwave emission from the same model and vary the kappa index such as to match the model radio brightness to the observed one.



## RESULTS

Below we show model microwave images for kappa indices 4, 20, and 32 and for the Maxwellian case. For small kappa, there are areas with deficit and excess of emission compared with observations. The best morphological agreement is achieved for  $\kappa = 20$ ; for larger  $\kappa$ , and for the Maxwellian case, an elongation of the main source towards the weaker source appears. We compare integrated brightness of the model source with the integrated observed brightness, and the peak brightness after the model convolution with the instrument beam with the brightness peak in the observed image below.



- I. Microwave gyroresonant emission is extraordinarily sensitive to the electron distribution type capable of distinguishing distributions with kappa indices up to about 100.
- II. For the AR analyzed here in detail we succeeded to constrain the kappa index to be certainly above 12 with the most likely value in the range 20–30, although higher values and the Maxwellian distribution might be consistent with the data as well.

This work is supported in part by NSF grant AGS-1250374, NASA grant NNX14AC87G.

## REFERENCES

Fleishman, G. D., Kuznetsov, A. A. ApJ 2014. V. 781. Id. 77; ApJ 2010. V. 721. P. 1127.  
Nita, G. M., Fleishman, G. D., Kuznetsov, A. A., Kontar, E. P., and Gary, D. E. ApJ 2015, 799, Id: 236.